International Journal of Science and Research (IJSR)
ISSN: 2319-7064
SJIF (2020): 7.803

Study of the Finite Plain Journal Bearing Considering Cavitation and Roughness Effect

Ganjar Kurnia[1], Mohammad Tauviqirrahman[1], Ojo Kurdi[1], Budi Setyana[1,2]

[1]Laboratory for Engineering Design and Tribology, Department of Mechanical Engineering, Diponegoro University, Semarang, Indonesia.

[2]Laboratory for Surface Technology and Tribology, Faculty of Engineering Technology, Twente University, Enschede, The Netherlands

E-mail: *ganjar12[at]gmail.com*

Abstract: ***Many studies have been performed on the impact of surface roughness on journal bearings, but there is still much to learn. Hydrodynamic lubrication has received far more attention than elastohydrodynamic lubrication. The effect of roughness and elastohydrodynamic lubrication on journal bearing cavitation will result in the lubricant and structural. This research will look into the effect of surface roughness on the pressure distribution, vapor volume fraction, and deformation of the journal bearing. The 2-way FSI approach, which is modeled with CFD, will be a helpful technique in this study. The simulation begins with the creation of a model in CAD and the determination of its geometry, meshing, phase definition, boundary conditions definition, and the determination of the Solution Method, the Solution Control, and the Iteration Process.The interaction of the lubrication fluid with the journal bearing's structure will be intriguing to see.It has been confirmed that as roughness increases, the pressure distribution, vapor volume fraction, von Mises stress, and deformation values decrease.***

Keywords: roughness, lubrication, bearing

1. Introduction

Bearing roughness has received much interest in recent years because of its opportunities to enhance tribological performance by lowering friction and wear and increasing load-carrying capacity. Roughness on the surface has been shown to improve the performance of tribological interactions in a variety of applications. One of the significant challenges is that the ideal roughness variables depend on the type of interaction and, more importantly, the operating conditions[1].Liang et al. [2]have been discovered that roughness at the lubricant inlet area can increase bearing performance, and that shallow dimples have a better effect than deep dimples. Microtextured surfaces have also been shown to improve bearing performance in some experiments [3]. The friction coefficient was reduced as a result of the roughness, with the maximum reduction of roughly 40% when compared to non-roughness samples, as shown by Galda et al.[4] in their research.

The process of creating and shattering air bubbles in liquids is known as cavitation. Cavitation happens when the fluid's static pressure drops below the vapor pressure of the liquid. Evaporation can occur not just when the temperature drops, but also when the pressure reduces. When the air bubbles reach a pressure higher than the vapor pressure, they will change back.When estimating the texture effect, it is critical to consider the cavitation phenomenon[5].As the pressure falls below the vapor pressure, air bubbles emerge in the cavitation area.When bearings are operated at higher speeds, a multiphase analysis of bearings with cavitation becomes particularly critical[6].Ausas et al. [7] explored the role of cavitation (negative pressure) on the numerical evaluation of journal bearing lubrication performance.When oil pressure rises on the convergent side of the bearing, these vapor bubbles rupture, resulting in high-intensity microjets [8].Yang et al.[9] discovered that the hydrodynamic plain bearing was severely harmed by cavitation wear as a result of flow instability.

In the modeling of lubrication difficulties, the handling of cavitation processes is crucial. To address this issue, many numerical methods have been devised. Oil supply cannot be estimated because mass is not preserved inside the cavitation area, but Reynolds conditions are the most extensively employed at the moment[10]. Cheng et al.[11]experiments found that a velocity-slip model that includes slip length within the cavitation area and slip boundary conditions at the liquid-gas boundaries can accurately determine the load capacity of a journal bearing.

Liu et al. [12] used CFD and modular FSI approaches to investigate thecavitation, center movement of the journal, and pressure distribution of an elastohydrodynamic lubrication issue [12].The maximum lubricant film pressure can generally be reduced due to elastohydrodynamic factors[13].A perturbation approach based on the Reynolds equation was used to compute the oil film pressure distribution, as well as the bearing dynamic stiffness and damping matrices. The bearing dynamic characteristics are determined by perturbing each node of the lubricant film domain, taking into consideration the impact of structural deformation in local bearings, journal tilting, and bending[14]. Other research looked into how a CFD method based on fluid-structure interaction(FSI)can accurately forecast the transient flow field of a misaligned journal bearing in a rotor-bearing system [15].Fluid film on journal bearings will be analyzed using the FSI (fluid-structure interaction) approach. The main purpose of this project is to find the impact of journal bearings roughness that undergo cavitation, with a focus on what happens to the cavitation area subsequently. Hydrodynamic pressure, vapor volume

fraction, von Mises stress,and shaft deformation caused by roughness applied to the housing and shaft are also investigated.

2. Methods

2.1 Theory

Many investigations use Reynolds or Stokes models, which ignore pressure gradients and inertia effects in the lubricating film. However, Arghir et al. [16]have shown that Navier-Stokes equations are ineffective for predicting pressure riseswhen macroroughness is present, as inertia effects might be significant. RANS (Reynolds averaged Navier-Stokes simulation) is a turbulent flow model that solves the Navier-Stokes equation over time. One of the RANS models used in fluent is the Two-Equation Model. The Reynold averaged Navier-Stokes simulation (RANS), which is commonly employed in Computational Fluid Dynamics to tackle a challenging 3D scenario, is replaced by the Two-Equation Model (CFD). In an incompressible viscous fluid, the RANS equation for determining film pressure is:

$$\frac{\partial}{\partial x_i}\left(\rho u_i u_j\right) = -\frac{\partial p}{\partial x_i} + \left[\mu\left(\frac{\partial u_i}{\partial x_j} + \frac{\partial u_j}{\partial x_i}\right)\right] + \frac{\partial}{\partial x_j}\left(-\rho\overline{u_i' u_j'}\right) \quad (1)$$

Czaban[17]looks at the impact of roughness on the factors involved, which necessitates the employment of statistical models. The Reynolds stochastic equation can be used to derive analytical considerations in the case of journal-bearing with hydrodynamic lubrication. The outcomes of the CFD simulation for hydrodynamic lubrication of conical bearings, considering the impacts of shaft and housing surface roughness, are shown. Roughness can be depicted as grain-sand roughness in this CFD simulation. Roughness height, for example, can be estimated (K_s). The following algorithm, as shown in equationseq. 2 and eq. 3, can be used to convert this parameter value to the arithmetic mean of surface roughness (R_a).

$$R_a = \frac{\pi K_s}{2}\left(\frac{\pi}{2} - \cos^{-1}\left(1 - \frac{\pi}{16}^2\right)^{\frac{1}{2}} - \frac{\pi}{2}\left(1 - \frac{\pi}{16}^2\right)^{\frac{1}{2}}\right) \quad (2)$$

$$K_s = 5.853\ R_a \quad (3)$$

The flow in cavitated areas was viewed as a two-phase lubricant and vapor/gas flow with uniform density, while the flow in the rest of the film was viewed as a compressible flow with constant bulk modulus[1]. To come up with a solution, the Schnerr-Sauer cavity model uses a derivation of the equation for mass transfer from a fluid to a vapor. The number of bubbles per volume of fluid is denoted by n_b. If no bubbles are created or destroyed, the bubble density will remain constant. The cavitation model's final equation is as follows:

$$If\ P \le P_v \rightarrow R = \frac{\rho_v \rho_l}{\rho}\alpha(1-\alpha)\frac{3}{R_b}\sqrt{\frac{2(P_v - P)}{3\rho_l}} \quad (4)$$

$$If\ P \ge P_v \rightarrow R = \frac{\rho_v \rho_l}{\rho}\alpha(1-\alpha)\frac{3}{R_b}\sqrt{\frac{2(P - P_v)}{3\rho_l}} \quad (5)$$

2.2 CFD Model

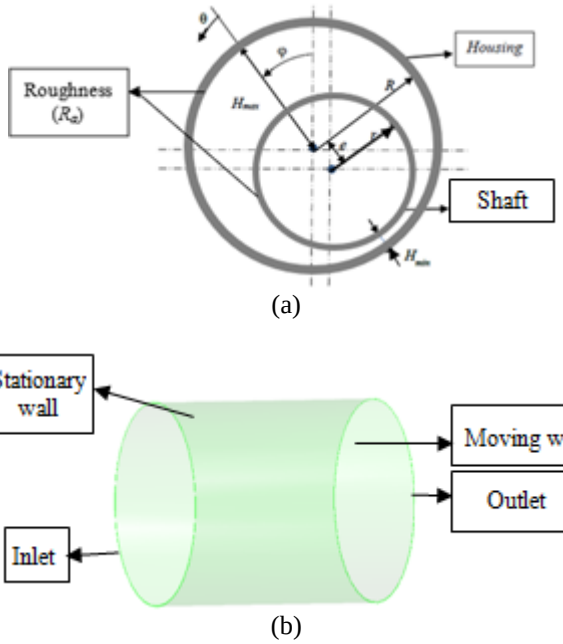

Figure 1: (a) Geometry journal bearing (b) boundary condition

The surface roughness of the outer shaft and inner bearing is modeled in this work. The lubrication mechanism is elastohydrodynamic lubrication, the fluid is Newtonian and incompressible, the turbulent flow model is k-epsilon, and the surface roughness is uniform sand-grain roughness, and the roughness parameter is utilized (R_a), the load applied is negligible, and there is no mention of the effect of displacement heat on lubrication. The dimensions of Figure 1 are as follows: the shaft radius is r = 50 mm, the housing radius is R = 50.145 mm, the bearing length L=133 mm, eccentricity ratio ε = 0.61, vapor viscosityρ_{sat}= 2 x 10^5 Pa.s, lubricant viscosity = 0.0127 Pa.s, vapor density η_{sat} = 1.2 kg/m^3, lubricant density ρ = 840 kg/m^3,maximum thickness fluid H_{max}= 0.23345 mm,minimum thickness film H_{min}= 0.05655 mm, roughness R_a= 0.2 µm, 0.8 µm, 3.2 µm, 25 µm,yield strength Y_s = 2.5 x 10^8Pa, andYoung's Modulus E = 2x 10^{11} Pa.

Four boundary conditions are used in this simulation: pressure input, pressure exit, moving wall, and stationary wall. Both the inlet and output pressures are set to zero. Concerning the bearing housing, the shaft is a moving wall with a rotational speed of n = 48.1 rad/s (stationary wall). The fluid is estimated using the finite volume method and CFD after all of the parameters have been entered. The SIMPLE technique is used to achieve an exact pressure for the velocity–pressure interaction. The momentum and volume fraction equations are discretized using a first-order upwind method. The spatial discretization of turbulent kinetic energy and turbulent dissipation rate is done using the first-order upwind discretization scheme.

2.3 Meshing

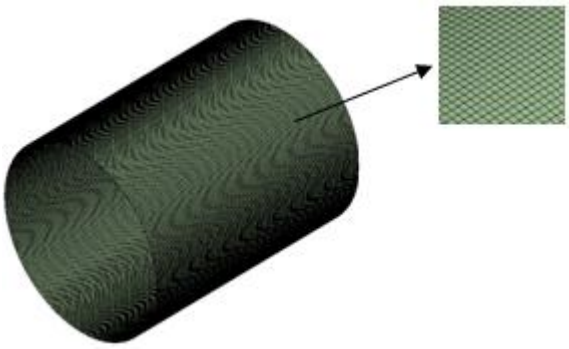

Figure 2: Meshing Models

To ensure that the parts are of good quality, the mesh used is a Hexahedral grid that is designed using the multizone, face sizing, and body sizing features. With a body sizing of 0.8 mm and a face sizing of 0.86 mm, the multizone is hexahedral, the multizone size is 0.095, the number of elements is 195216, the number of nodes is 261856, the maximum skewness value is 0.42061, the minimum skewness value is2.4721 x 10^{-3} and the average skewness value is 4.4796 x 10^{-2}. Because the skewness in this modeling is 0.4206, the mesh quality is good, and it may generate good computational quality.The better the data transfer between the meshes, the less skewed it is. When an element is skewed, it requires a lot of correction when computing, which decreases the quality of the computation and slows down the process.

3. Result and Discussion

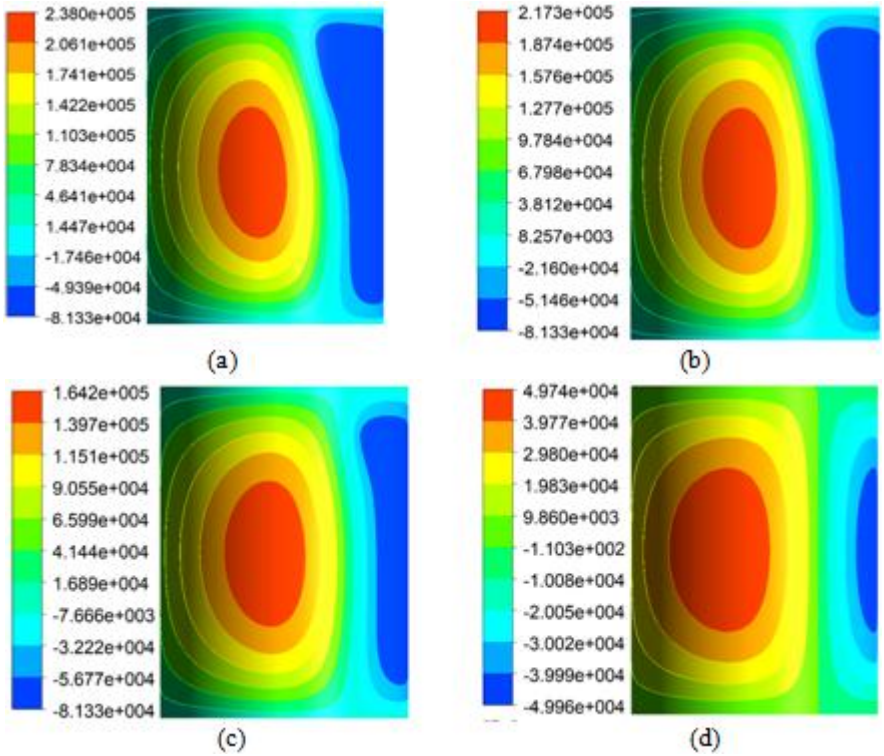

Figure 3: Hydrodynamic pressure on a fluid film (Pa)*;* a) R_a= 0.2 µm, b) R_a= 0.8 µm, c) R_a= 3.2 µm, d) R_a= 25 µm

The maximum pressure falls as the roughness increases, as shown in the graph above. The maximum pressure for roughness 0.2 µm is 2.380 x 10^5Pa, for roughness 0.8 µm it is 2.173 x 10^5 Pa, for roughness 3.2 µm it is 1.642 x 10^5 Pa, and for roughness 25 µm it is 4.974 x 10^4Pa. Because of the pressure drop generated by the roughness on the surface,the cross-sectional area in contact with the fluid will be bigger with a constant normal force, resulting in a smaller pressure. The oil film pressure, carrying capacity, and friction can all be reduced by roughness, according to a study by Verma et al. [18]. The wedging effect on the pressurized fluid film will be broken due to the reduced pressure caused by surface roughness.As a result, it's crucial to focus on the provision of surface roughness, as it can have an impact on the size of the pressure that happens. As a result, the lower the pressure, the rougher the bearing. The better the journal bearing friction force performance, the lower the pressure. Because the lubricant is under less pressure, the distance between the cavities is growing longer and the frictional force is decreasing. However, as the roughness rises, the weight carrying capacity's performance deteriorates.

The smoother the surface, the greater the pressure on the lubricant, as shown in the graph. At a roughness of 0.2µm, the largest maximum pressure occurs, while at a roughness of 25 µm, the smallest pressure occurs. The minimum pressure at each roughness value is -8.13 x 10^4 Pa, which is nearly identical. The negative symbol denotes the bearing's lowest operating pressure below atmospheric pressure. One of the reasons for cavitation is negative pressure. The fluid in the cavitation area comprises vapor or air bubbles and lubricating oil, as the fluid in the cavitation area decreases the pressure. Air bubbles develop in this cavitation area.As the surface roughness rises, the appearance of this cavitation reduces. The pressure does not change -8.13 x 10^4Pa, as shown in the pressure distribution diagram above. As the

roughness increases, the minimum stress area (horizontal line) shrinks. This means that fewer vapors/air bubbles are present. Because the pressure drop is still above the vapor pressure for roughness 25 µm, no cavitation occurs, and no lubricant converts to vapor.As a result, it may be argued that the greater the surface roughness, the smaller the cavitation area or the absence of cavitation.Figure 4, which depicts the cavitation area and fraction volume, provides more information.

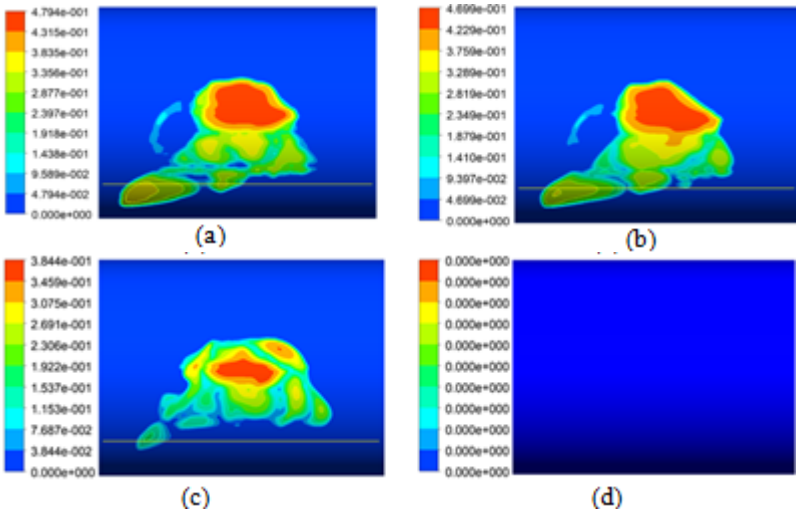

Figure 4. Contour of vapor fraction volume on fluid film1 a) R_a= 0.2 µm, b) R_a= 0.8 µm, c) R_a= 3.2 µm, d) R_a= 25 µm.

It can be seen that the volume of vapor fraction that occurs in the cavitation area in the form of vapor or air bubbles ranges from 0 percent to 47.9 percent. A condition happens when the amount of lubricating fluid diminishes and bubbles emerge in the area where there is a volume fraction, or in other words, lubricant starvation.

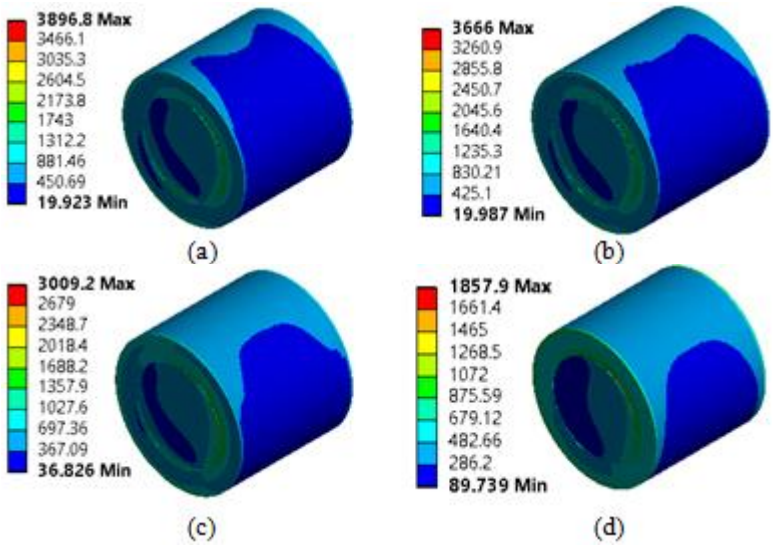

Figure 5: Von Mises stress (Pa)*;* a) R_a= 0.2 µm, b) R_a= 0.8 µm, c) R_a= 3.2 µm, d) R_a= 25 µm.

The von Mises stress in the shaft and housing decreases as the roughness increases, as shown in the diagram above. This is due to the interaction of the fluid pressure between the shaft and the housing. As a result, the von Mises stress increases as the fluid pressure increases. Both the shaft and the housing are deformed as a result of this stress

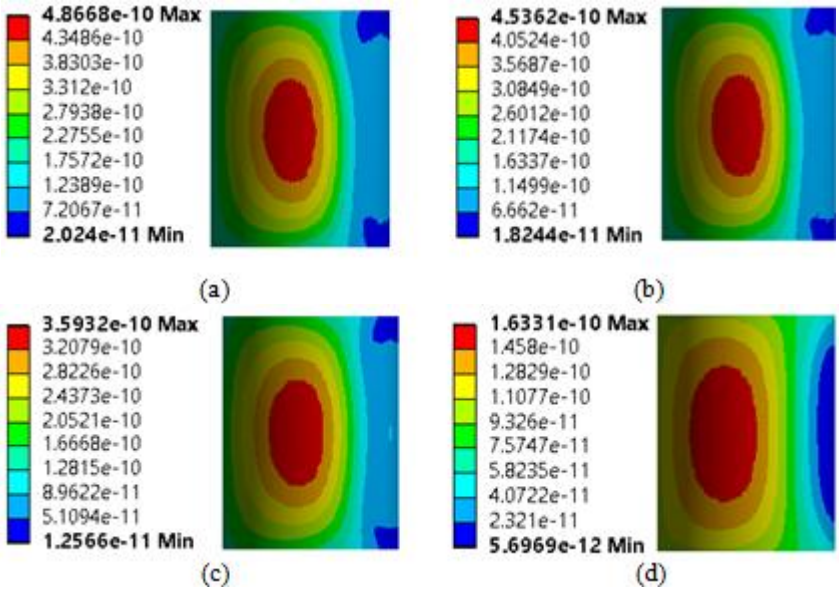

Figure 6: Deformation (m) on shaft; a) R_a= 0.2 µm, b) R_a= 0.8 µm, c) R_a= 3.2 µm, d) R_a= 25 µm.

It can be shown that as the surface roughness rises, the deformation reduces. This is because when the roughness increases, the stress that happens decreases. Because the distortion is significantly smaller than the high asperity and clearance in this scenario, there is no friction due to deformation.There are obvious variations in the film pressure distribution, the maximum film pressure, the film thickness distribution, and the least film thickness distribution when the journal in the bearing area becomes misaligned due to shaft deformation.The location of the maximum film pressure travels towards the end plane of bearing as the angle of misalignment grows; at the same time, the value of the maximumhydrodynamic pressure rises [19].

4. Conclusion

Modeling of journal bearings with cavitation has been completed successfully. The elastic deformation of the shaft, as well as the hydrodynamic pressure and vapor volume percentage in the fluid layer, are calculated. The hydrodynamic pressures are affected by roughness and cavitation, which will impair the journal bearing performance subsequently. In addition, steam emits from the lubricant in the cavitation area, ranging from 0 percent to 47.9 percent. With increased shaft and housing roughness, the von mises stress that arises diminishes.When compared to the housing, the shaft experiences the most deformation, yet it is still an elastic deformation.

References

[1] Gropper D, Wang L, Harvey TJ. Hydrodynamic lubrication of textured surfaces: A review of modeling techniques and key findings. Tribol Int. 2016;94:509–29.
[2] Liang X, Liu Z, Wang H, Zhou X, Zhou X. Hydrodynamic lubrication of partial textured sliding journal bearing based on three-dimensional CFD. Ind Lubr Tribol. 2016;68:106–15.
[3] Chen H, Chen D, Li Y. Investigation on effect of surface roughness pattern to drag force reduction using rotary rheometer. J Tribol. 2006;128:131–8.
[4] Galda L, Sep J, Prucnal S. The effect of dimples geometry in the sliding surface on the tribological properties under starved lubrication conditions. Tribol Int [Internet]. Elsevier; 2016;99:77–84. Available from: http://dx.doi.org/10.1016/j.triboint.2016.03.015
[5] Gherca AR, Maspeyrot P, Hajjam M, Fatu A. Influence of texture geometry on the hydrodynamic performances of parallel bearings. Tribol Trans. 2013;56:321–32.
[6] Dhande DY, Pande DW. Multiphase flow analysis of hydrodynamic journal bearing using CFD coupled Fluid Structure Interaction considering cavitation. J King Saud Univ - Eng Sci [Internet]. King Saud University; 2018;30:345–54. Available from: http://dx.doi.org/10.1016/j.jksues.2016.09.001
[7] Ausas R, Ragot P, Leiva J, Jai M, Bayada G, Buscaglia GC. The impact of the cavitation model in the analysis of microtextured lubricated journal bearings. J Tribol. 2007;129:868–75.
[8] Garner DR, James RD, Warriner JE. Cavitation Erosion Damage in Engine Bearings: Theory and Practice. Am Soc Mech Eng. 1980;102:847–57.
[9] Moreno DP, Yang MC, Hernández AA, Linsey JS, Wood KL. A Step Beyond to Overcome Design Fixation: A Design-by-Analogy Approach. Des Comput Cogn '14. 2015.
[10] SWIFT HW. the Stability of Lubricating Films in Journal Bearings. (Includes Appendix). Minutes Proc Inst Civ Eng. 1932;233:267–88.
[11] Cheng F, Ji W. A velocity-slip model for analysis of the fluid film in the cavitation region of a journal bearing. Tribol Int. 2016;97:163–72.
[12] Liu H, Xu H, Ellison PJ, Jin Z. Application of computational fluid dynamics and fluid-structure interaction method to the lubrication study of a rotor-bearing system. Tribol Lett. 2010;38:325–36.
[13] Xu H. Elastohydrodynamic lubrication in plain bearings. Tribol Ser. 1997;32:641–50.
[14] Ebrat O, Mourelatos ZP, Vlahopoulos N, Vaidyanathan K. Calculation of journal bearing

dynamic characteristics including journal misalignment and bearing structural deformation©. Tribol Trans. 2004;47:94–102.
[15] Li Q, Liu SL, Pan XH, Zheng SY. A new method for studying the 3D transient flow of misaligned journal bearings in flexible rotor-bearing systems. J Zhejiang Univ Sci A. 2012;13:293–310.
[16] Arghir M, Roucou N, Helene M, Frene I. Theoretical analysis of the incompressible laminar flow in a macro-roughness cell. J Tribol. 2003;125:309–18.
[17] Czaban A. Cfd Analysis of Hydrodynamic Lubrication of Slide Conical Bearing With Consideration of the Bearing Shaft and Sleeve Surface Roughness. J KONES Powertrain Transp. 2014;21:35–40.
[18] Verma S, Kumar V, Gupta KD. Performance analysis of flexible multirecess hydrostatic journal bearing operating with micropolar lubricant. Lubr Sci. 2012;24:273–92.
[19] Sun J, Changlin G. Hydrodynamic lubrication analysis of journal bearing considering misalignment caused by shaft deformation. Tribol Int. 2004;37:841–8.